Time-varying pulmonary arterial compliance

BRYDON J. B. GRANT, JAMES M. FITZPATRICK, AND BARUCH B. LIEBER
Departments of Medicine and Mechanical and Aerospace Engineering, State University of New York at Buffalo, Buffalo, New York 14215

GRANT, BRYDON J. B., JAMES M. FITZPATRICK, AND BARUCH B. LIEBER. *Time-varying pulmonary arterial compliance.* J. Appl. Physiol. 70(2): 575–583, 1991.—We tested the hypothesis that pulmonary arterial compliance (Ca) varies during the ventilatory cycle. Pressure and flow in the main pulmonary artery were measured in open-chest dogs under chloralose anesthesia ($n = 12$) with a positive-pressure volume-cycled ventilator. Input impedance was calculated from the pressure and flow waves of heart cycles obtained immediately after the start of inspiration (SI) and immediately after the start of expiration (SE). A lumped parameter model was used to calculate Ca from the input impedance spectrum of the main pulmonary artery. Three levels of positive end-expiratory pressure (PEEP) were used before and after meclofenamate ($n = 6$) or vagotomy ($n = 6$). Ca was significantly greater at SE than at SI at each level of PEEP. PEEP increased Ca at SE but not at SI. None of these changes was altered by meclofenamate or vagotomy, suggesting that these differences of Ca were due to passive mechanical effects rather than an active neurohumoral mechanism. We conclude that Ca is time varying during the ventilatory cycle because it is altered by the dynamic increase of lung volume between SI and SE, but not with the quasi-static increase of lung volume induced by raising the level of PEEP. These changes of Ca were unaffected by vagal feedback or inhibition of cyclooxygenase. We suggest that the increased Ca just after the start of expiration may result from dynamic shifts of blood volume from the extra-alveolar to the alveolar vessels.

input impedance; positive end-expiratory pressure; characteristic impedance; ventilatory cycle; time-varying compliance

THERE ARE TWO COMPONENTS to blood flow in the pulmonary circulation: mean flow and pulsatile flow. Mean flow is opposed by the resistive properties of the pulmonary circulation; pulsatile flow is opposed by its inertial and compliant properties. Pulmonary vascular resistance represents the opposition to the mean components of flow. The input impedance spectrum provides a more complete description of right ventricular afterload than resistance alone because it represents the opposition to both the mean and pulsatile components of flow (13). It is generally accepted that respiration affects pulmonary vascular resistance (5). In contrast, previous reports suggest that there is no significant effect on the impedance, which represents the opposition to the pulsatile components of flow (3, 15). Nevertheless, there are several potential mechanisms that may alter the dimensions and/or the elasticity of the proximal pulmonary arteries, which have properties that determine input impedance. First, there are respiratory fluctuations of pulmonary arterial pressure (PAP). PAP has been shown to alter the dimensions of proximal pulmonary arteries and increase pulmonary arterial compliance (Ca) (7). Second, vagal pathways mediate the reflex effects of lung distension on tracheal smooth muscle tone (19). There may be similar effects on pulmonary arterial smooth muscle. Third, lung inflation releases cyclooxygenase products, which alter compliance of the lung parenchyma (1) and therefore may also affect compliance of the pulmonary arteries.

Recently, we showed that on statistical grounds at least three components are needed to describe the pulmonary arterial input impedance spectrum (Z_i): a resistance (Rin), which represents input resistance and is defined as mean PAP divided by mean pulmonary arterial flow; a resistor, which represents characteristic impedance (Z_c); and a capacitor, which represents Ca (8). Previous authors have tended to express the changes of Z_i in terms of Rin and Z_c and may have missed changes of Ca. In the present study we used a lumped parameter model to calculate not only Rin and Z_c but also Ca to provide a more complete description of the right ventricular afterload.

METHODS

Animal preparation. Experiments were performed on 12 mongrel dogs that weighed between 17 and 21 kg. Anesthesia was induced with thiamylal (1.5 mg/kg) followed immediately by intravenous injection of 2 ml/kg body weight of a chloralose solution (6 g/dl α-chloralose, 4.6 g/dl sodium tetraborate, and 5 g/dl sodium bicarbonate). Anesthesia was maintained with a continuous infusion of a 1:1.85 dilution of that solution at a rate of 1.32 $ml \cdot kg^{-1} \cdot h^{-1}$. The dogs were intubated and ventilated with a volume-cycled pump (model 681, Harvard Apparatus, Natick, MA). Intravenous pancuronium bromide (0.1 mg/kg) was used for muscular paralysis. The dogs were ventilated at a respiratory rate of 12–15 min^{-1} with a constant tidal volume throughout each experiment. Stroke volume of the ventilator was set at ~15 ml/kg. Inspiration was achieved by positive pressure; expiration was passive. The inspiratory and expiratory times were fixed and equal. Airway gas fractions were monitored with a Perkin-Elmer mass spectrometer. The ventilator settings were adjusted to obtain an end-tidal P_{CO_2} of 5%. Airway pressure was monitored with a Validyne differential pressure transducer. A catheter was placed in the right femoral artery to monitor systemic

arterial pressure with a Statham P23 ID pressure transducer.

A left thoracotomy was performed in the fifth intercostal space, and 5 cmH_2O of positive end-expiratory pressure (PEEP) was applied to prevent atelectasis. The pericardium was then transected vertically, and the pulmonary artery was isolated by blunt dissection. A Statham electromagnetic flow probe (between 16 and 18 mm ID) was placed around the main pulmonary artery. Two 3F micromanometer-tipped catheters (Millar, Houston, TX) were placed, through purse-string sutures, into the right ventricular outflow tract and into the pulmonary artery for simultaneous pressure measurements. All pressure calibrations were zeroed relative to atmosphere; no correction was made for the height of the pressure transducer from the right atrium.

Experimental protocol. After instrumentation, data collection was started when the preparation was judged to be stable as manifested by constant mean systemic arterial pressure, PAP, and flow ($\dot{Q}$). In all dogs, measurements were collected over a period of 10 breaths at 5, 10, and 15 cmH_2O PEEP. In six dogs, this protocol was repeated 30 min after meclofenamate administration (3 mg/kg iv). In the other six dogs this protocol was repeated after the administration of atropine (0.1 mg/kg) and bilateral cervical vagotomy. Atropine was given before vagotomy to avoid the effects of vagal efferent stimulation that might occur when the vagi are cut.

Data collection and analysis. All electrical analog signals were displayed on an eight-channel Gould 2800S recorder. These analog signals were converted to digital form (Data Translation DT2801A) and recorded in parallel on a computer (Wells-American A Star, Columbia, SC). The pressure and flow waves were sampled at 500 Hz per channel. The ventilatory cycle was defined from the output of a microswitch, which was positioned on the ventilator to deliver a 5-V pulse at end expiration. End inspiration was defined as the midpoint between two end-expiratory pulses because the inspiratory and expiratory times were equal. The start and finish of individual heart cycles were defined from a pulse triggered by the QRS complex of the electrocardiogram (ECG/Biotach amplifier, Gould). Two sets of heart cycles were selected at different phases of the ventilatory cycle. Each set consisted of 10 cardiac cycles selected from successive breaths. One set was composed of the first complete cardiac cycle that occurred immediately after end expiration, which is the start of inspiration (SI). The other set was composed of the first complete cardiac cycle that occurred immediately after end inspiration, which is the start of expiration (SE). An example of the selection of cardiac cycles at SI and SE is shown in Fig. 1. The data obtained during these cardiac cycles were used to calculate heart rate (HR), right ventricular end-diastolic pressure (RVEDP), and the mean values of PAP, $\dot{Q}$, airway pressure, systemic arterial blood pressure (BP), and stroke volume (SV) at SI and SE. Input impedance was calculated by Fourier analysis for each of the 10 cardiac cycles. A mean value and its variance were calculated at zero frequency and at each harmonic for both the real and imaginary components. A lumped parameter model was used to calculate characteristic impedance and pulmonary arterial compliance.

Estimation of characteristic impedance and pulmonary arterial compliance. Details of the procedure to calculate Z_c and Ca have been described elsewhere (8). In that study, we tested the ability of a number of different lumped parameter models to recover values of Z_c and Ca. Because each model yields different estimates of Z_c and Ca, we used the same lumped parameter model throughout the present study. Although using the same lumped parameter model does not provide necessarily the most efficient fit to the data in the statistical sense for every data set, it does provide consistency in our estimation of the parameters. The electrical representation of the lumped parameter model has four components and is the same model that we have used previously (6). A resistor (Z_c) is in series with a capacitor (Ca) and an inductor. A second resistor (Rin) is in parallel with Z_c and Ca. Z_c represents characteristic impedance, Ca represents pulmonary arterial compliance, and Rin represents pulmonary input resistance. The physiological correlate of the inductor in the lumped parameter model is unknown; most of the inertial properties of pulmonary arterial input impedance are contained within characteristic impedance. Because the parameter estimate of the inductor was zero in 45% of occasions, its values are not reported here.

Parameter values were varied with the Marquardt technique until the model impedance was similar to the measured impedance spectrum measured experimentally according to the maximum likelihood criterion with chi-squared minimization. Iterations were stopped when the weighted residual sum of squares changed by $<0.0001\%$ with successive iterations. The degree of interdependence between the parameter estimates was investigated in one experiment by a Monte Carlo technique (17). For each impedance spectrum, 100 impedance spectra were synthesized from the mean and variance of the real and imaginary components at zero frequency and each harmonic. New mean values were randomly generated based on the assumption of a normal distribution of measurement errors. The lumped parameter model was fitted to each of the synthesized spectra, and the resulting group of parameter values was used to estimate the correlation coefficient.

Statistical analysis. Analysis of variance for repeated measurements was used for statistical assessment. A logarithmic transformation was used for Z_c and Ca. On the data obtained before the intervention (meclofenamate or vagotomy), we tested for the effect of respiration, an effect due to differences in the level of PEEP, and an interaction term to test the effect of PEEP on the hemodynamic response to respiration. To determine the effect of meclofenamate and vagotomy on the hemodynamic response to ventilation and PEEP, we analyzed each series of experiments separately. Statistical significance was accepted at the 5% level.

RESULTS

The primary disturbance to the pulmonary circulation was an increase in lung volume due to inspiration or

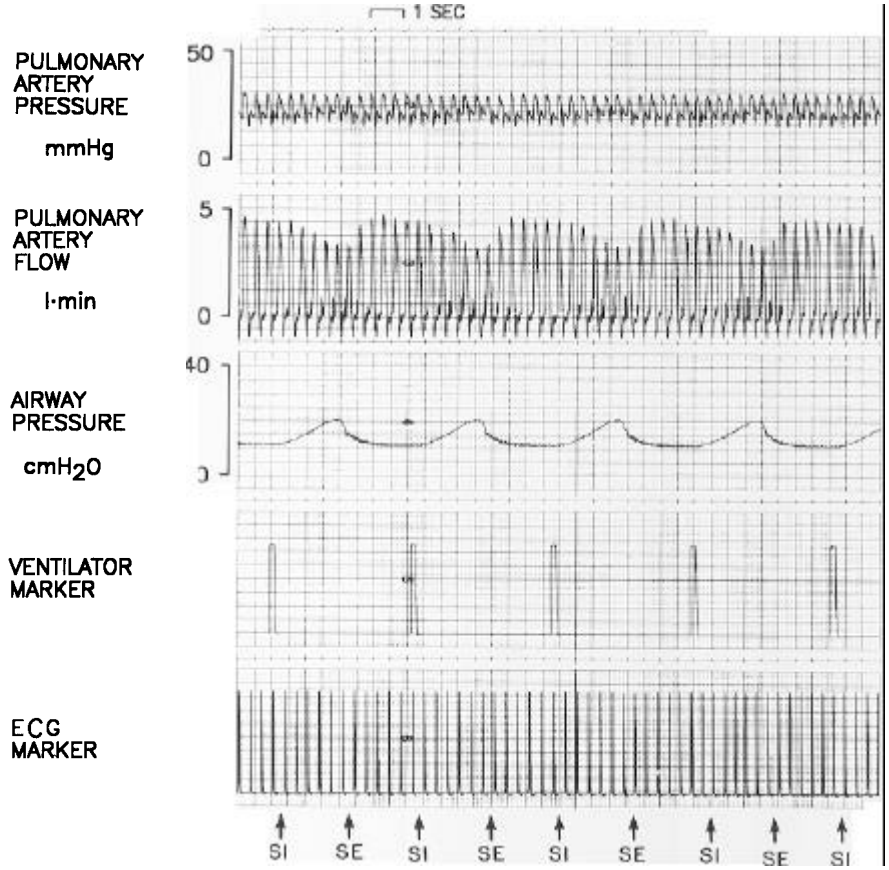

FIG. 1. Chart recording of pulmonary arterial pressure, blood flow, airway pressure, ventilator signal marking end expiration, and ECG signal marking occurrence of QRS complex. SI, cardiac cycles selected at start of inspiration; SE, cardiac cycles selected at start of expiration.

increased levels of PEEP. Changes of lung volume are reflected in the changes of airway pressure. Airway pressure increased with inspiration (from SI to SE) because the lungs are ventilated with positive pressure. Airway pressure increased from 6.3 ± 0.2 to 8.0 ± 0.3 (SE) cmH_2O at 5 cmH_2O PEEP, from 10.9 ± 0.2 to 13.7 ± 0.3 cmH_2O at 10 cmH_2O PEEP, and from 15.7 ± 0.2 to 19.6 ± 0.3 cmH_2O at 15 cmH_2O PEEP. Not surprisingly, there was a significant increase in airway pressure due to both ventilation ($P < 0.0001$) and PEEP ($P < 0.0001$). In addition, there is a significant interaction effect due to an increase in airway pressure with inspiration as the level of PEEP is increased ($P < 0.0001$). The chest is open in this preparation; therefore pleural pressure is atmospheric, airway pressure is transpulmonary pressure, and PAP and RVEDP are transmural pressures. Because the ventilator was a volume-cycled pump, it delivers a similar tidal volume at all levels of PEEP. Therefore, the increase in airway pressure between SI and SE with increasing levels of PEEP is probably due to the reduced lung distensibility as lung volume increases.

Effect of ventilation on hemodynamics. Figure 2 shows the changes in Rin with ventilation and PEEP. The changes of Rin mirror the increases in airway pressure. Rin increases with inspiration and PEEP, and the increase with inspiration is potentiated by increasing the level of PEEP. Changes of Rin may result from alterations of mean PAP, mean $\dot{Q}$, or both. The changes of PAP, $\dot{Q}$, Z_c, and Ca with respiration at the three levels of PEEP are shown in Fig. 3. Although there were no significant changes of PAP with inspiration, there was a significant decrease in $\dot{Q}$ between SI and SE. PEEP significantly increased PAP and decreased $\dot{Q}$.

Although ventilation had no effect on Z_c, there was a small significant decrease in Z_c with PEEP. Ca was significantly greater at SE than at SI at all three levels of

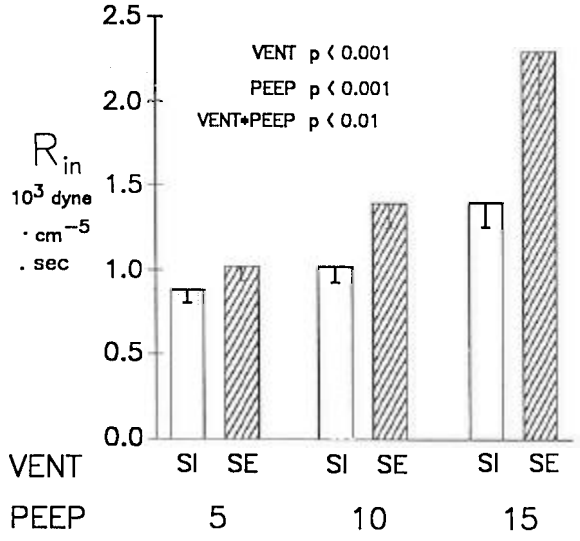

FIG. 2. Comparison of mean pulmonary arterial input resistance (Rin) at different phases of ventilation (VENT), start of inspiration (SI, open bars) and start of expiration (SE, hatched bars), at 3 levels of positive end-expiratory pressure (PEEP, cmH_2O). Error bars, SE (n = 12 dogs).

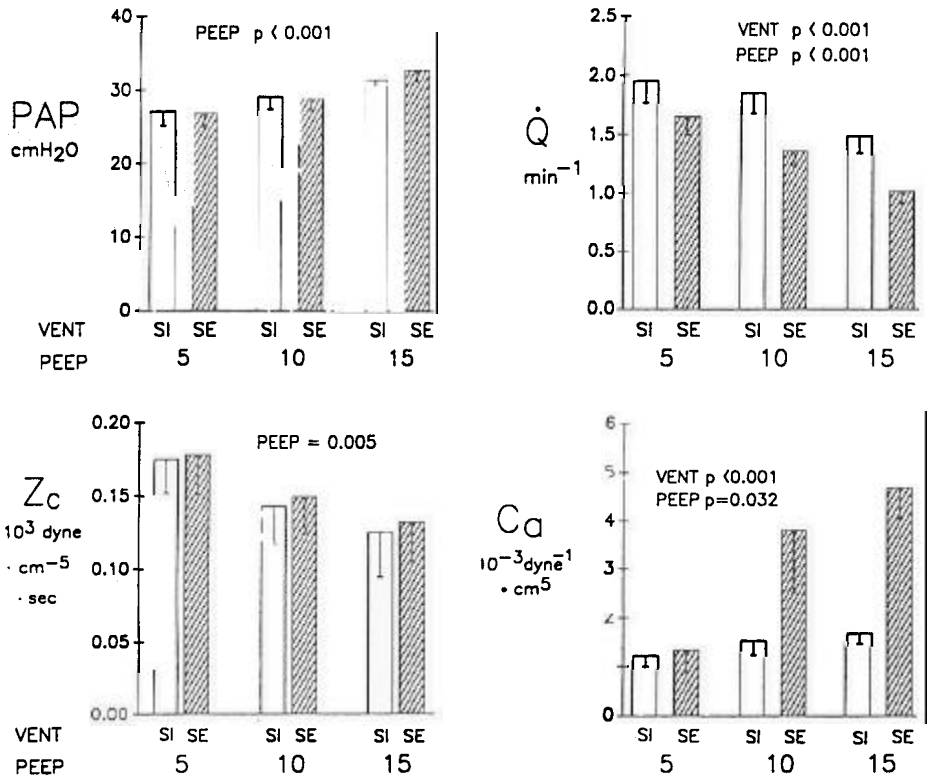

FIG. 3. Comparison of mean pulmonary arterial pressure (PAP), characteristic impedance (Z_c), pulmonary arterial flow ($\dot{Q}$), and pulmonary arterial compliance (Ca) at different phases of ventilation (VENT) and levels of PEEP. Other symbols are as defined in Fig. 2 legend.

PEEP. Although there was marked variation in the values for Ca between dogs, a greater value of Ca at SE than at SI was observed consistently at each of the three levels of PEEP. A greater Ca at SE occurred in 10 of 11 comparisons at 5 cmH_2O PEEP and 9 of 10 comparisons at both 10 and 15 cmH_2O PEEP. Not all 12 comparisons could be made at each of the three levels of PEEP because the lumped parameter model did not always converge to finite values of Ca. The increase of Ca with PEEP only occurred at SE ($P < 0.03$) and not at SI ($P > 0.6$). Because of the marked variance of Ca, the magnitude of the increase of Ca between SI and SE is not well defined. The percent increase of Ca at SE from SI was +9% (95% confidence limits: −27 to +62%) at 5 cmH_2O PEEP, +127% (95% confidence limits: +49 to +247%) at 10 cmH_2O PEEP, and +169% (95% confidence limits: +73 to +247%) at 15 cmH_2O PEEP.

These values of Z_c and Ca were calculated from the impedance spectrum. There are some potential difficulties that can occur when the impedance spectrum is calculated from single cardiac cycles at different phases of the ventilatory cycle. Differences between the beginning and the end of the pressure wave during one cardiac cycle can cause a sharp discontinuity that results in the addition of high-frequency components. The Fourier representation of this discontinuity results in leakage of this high-frequency component into the moduli of the impedance spectrum at lower frequencies of the spectrum (2). As a result, leakage could cause an increase in Z_c. We were concerned that leakage might occur at SE when rapid changes of transpulmonary pressure and lung volume occurred at that moment in the ventilatory cycle. There were, however, no significant differences between Z_c at SI and SE. In addition, we applied a Hanning taper, which removes any discontinuity at the beginning and end of the cycle by weighting the pressure and flow waves with a cosine function (2), but we still found that Ca was statistically significantly greater at SE than SI.

Another concern was that the increase in Ca occurred as a result of the increase in Rin. Previously, we have reported that there is a degree of interdependence between the model parameters (7). In the present study, we calculated the correlation coefficients between Rin and Ca to range between 0.11 and 0.72. Therefore, increases in Ca were associated with increases in Rin. To verify that this correlation is not exclusively responsible for the increase in Ca, the zero-frequency term at SE was adjusted to be the same as at SI and thus maintained Rin constant between SI and SE. Even under these conditions we found that Ca was greater at SE than at SI in 9 of 11 occasions at 5 cmH_2O PEEP, in 8 of 10 occasions at 10 cmH_2O PEEP, and in 7 of 9 occasions at 15 cmH_2O PEEP.

The decline of $\dot{Q}$ with inspiration and with increased levels of PEEP was associated with an increase of RVEDP and a decrease of SV (Fig. 4). Because the chest is open, RVEDP is essentially a transmural pressure. HR increased and BP decreased with PEEP, but neither changed between SI and SE.

Effect of meclofenamate on hemodynamics. Table 1 shows the effects of meclofenamate on hemodynamic variables and on their response to ventilation and PEEP. The administration of meclofenamate did cause a small but significant decrease in HR and an increase in BP, but it had no significant effect on the changes of

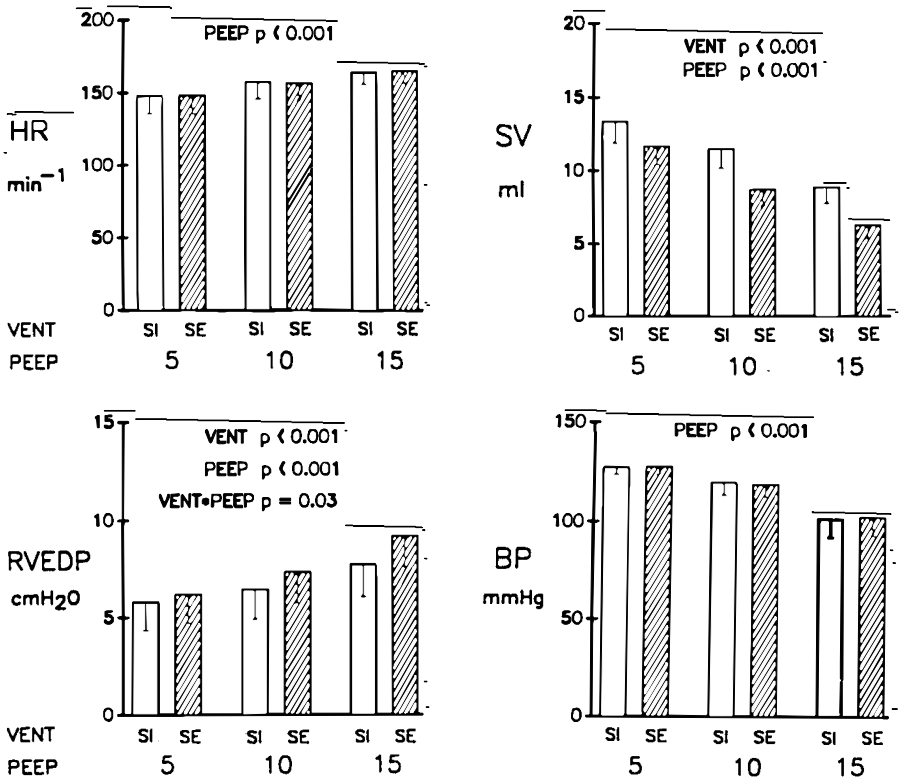

FIG. 4. Comparison of mean heart rate (HR), right ventricular end-diastolic pressure (RVEDP), stroke volume (SV), and systemic arterial blood pressure (BP) at different phases of ventilation (VENT) and levels of PEEP. Other symbols are as defined in Fig. 2 legend.

PAP, $\dot{Q}$, Z_c, Ca, RVEDP, or SV. Meclofenamate had no significant effects on the differences of Ca or between SI and SE or on the hemodynamic response to PEEP.

Effect of vagotomy on the hemodynamics. Table 2 shows the effects of vagotomy on hemodynamic variables and on their response to ventilation and PEEP. Vagotomy caused small but significant increases of PAP, RVEDP, HR, and BP. Although vagotomy had no significant effect on the differences of Ca or between SI and SE, it does alter the effects of PEEP. After vagotomy, there was less of a decrease of BP, SV, and mean $\dot{Q}$ with PEEP. This effect of vagotomy was statistically significant. Associated with the smaller decrease of $\dot{Q}$, there was a significantly greater increase of PAP with PEEP after vagotomy.

DISCUSSION

Comparison of our results to others. The effects of PEEP on hemodynamics that occurred in these experiments were similar to results reported by others. The results of Pouleur et al. (18) and our results show that PEEP increases mean PAP and decreases mean $\dot{Q}$, Z_c, SV, and BP. Calvin et al. (3) showed corresponding changes of mean PAP, mean $\dot{Q}$, RVEDP, and SV with PEEP to our results, although they did not detect a change of Z_c with PEEP. In a previous smaller study of eight comparisons (6), we also were unable to detect a significant effect of PEEP on Z_c. Our results are consistent with results obtained by Baier et al. (1), who concluded that cyclooxygenase inhibition did not affect the changes of mean PAP and cardiac output with PEEP (1). Cassidy et al. (4) suggested that PEEP causes reflex cardiovascular depression. Our study supports their conclusion because there was less of a decrease of BP and SV with PEEP after vagotomy.

Measurement of pulmonary arterial compliance. Ca was calculated from the impedance spectrum with a lumped parameter model. Our values of Ca are of the same order as those obtained by Van den Bos et al. (20), who also used a lumped parameter model to estimate Ca [1.8 ± 0.4 (SE) 10^{-3} $dyn^{-1} \cdot cm^5$]. This bias is appropriate for our study because we were interested in the effects of ventilation on right ventricular afterload, which is determined primarily by input impedance (13). A problem with all lumped parameter models is that a change in parameter value could result from a spurious factor. We have tested for two potential problems, namely, leakage and parameter correlation, but neither could account for the Ca being greater at SE than at SI. The magnitude of the increase of Ca, however, may have been exaggerated to some extent by parameter correlation between Rin and Ca.

Increase of pulmonary arterial compliance with inspiration. There were no significant differences in mean PAP between SI and SE. Therefore, the increase of Ca between SI and SE cannot be due to differences in pressure that may have altered vascular geometry (7). Ca was not affected significantly by the quasi-static lung volume changes at SI. We conclude that the increase in Ca after inspiration cannot be explained by an increase in lung volume altering vascular geometry. Ca is calculated from oscillatory pressure and flow, which are harmonics of HR. Therefore, variations of Ca could be due to frequency dependence of compliance. This possibility can be discounted because there was no significant dif-

TABLE 1. *Effect of meclofenamate on hemodynamic variables and their response to ventilation and positive end-expiratory pressure*

Hemodynamic Variables	Phase of Ventilation						Effect of Meclofenamate			
	Start of inspiration, cmH_2O PEEP			Start of expiration, cmH_2O PEEP						
	5	10	15	5	10	15	M	M* VENT	M* PEEP	
PAP, cmH_2O										
B	24±2	26±2	29±2	24±2	27±2	31±2	NS	NS	NS	72
A	25±2	27±2	30±2	24±2	27±2	31±2				
$\dot{Q}$, l/min										
B	2.1±0.5	1.9±0.4	1.7±0.3	1.8±0.4	1.6±0.3	1.3±0.2	NS	NS	NS	72
A	2.2±0.5	2.1±0.5	1.7±0.3	1.8±0.4	1.5±0.3	1.1±0.2				
Z_c, $dyn \cdot cm^{-5} \cdot s$										
B	168 + 67 − 48	138 + 63 − 43	110 + 65 − 41	171 + 58 − 44	125 + 63 − 42	92 + 69 − 39	NS	NS	NS	69
A	143 + 67 − 46	138 + 68 − 46	135 + 63 − 43	138 + 63 − 43	124 ± 72 − 45	154 + 72 − 49				
Ca, 10^{-5} $dyn^{-1} \cdot cm^5$										
B	1.5 + 0.3 − 0.3	1.6 + 0.3 − .03	2.3 + 0.6 − 0.5	1.8 + 0.5 − 0.4	3.4 + 1.8 − 0.2	3.9 + 1.1 − 0.9	NS	NS	NS	61
A	3.2 + 2.1 − 1.3	1.7 + 1.0 − 0.6	1.6 + 1.0 − 0.6	3.3 ± 1.9 − 1.2	4.4 + 2.8 − 1.7	1.8 + 0.9 − 0.6				
RVEDP, cmH_2O										
B	5±1	6±1	7±2	6±2	6±2	8±2	NS	NS	NS	72
A	6±2	6±1	7±1	6±1	7±1	8±1				
HR, min^{-1}										
B	149±24	155±23	168±16	149±25	154±23	168±16	0.002	NS	NS	72
A	124±11	141±14	160±12	123±10	139±14	158±12				
BP, mmHg										
B	129±6	126±7	115±9	130±6	126±7	116±9	<0.0001	NS	NS	72
A	145±9	141±9	134±10	147±9	142±9	135±1				
SV, ml										
B	15±2	13±2	10±1	13±2	10±1	8±1	NS	NS	NS	72
A	17±3	14±2	10±1	14±2	11±2	7±8				

Values are means ± SE and are given for before (B) and after (A) meclofenamate. PAP, mean pulmonary arterial pressure; $\dot{Q}$, mean pulmonary arterial blood flow; Z_c, characteristic impedance; Ca, pulmonary arterial compliance; RVEDP, right ventricular end-diastolic pressure; HR, heart rate; BP, femoral arterial blood pressure; SV, stroke volume. *P* values are given for effect of meclofenamate (M), effect of meclofenamate on response to ventilation (M*VENT), and effect of meclofenamate on response to positive end-expiratory pressure (M*PEEP); *n*, no. of data points.

ference in HR between SI and SE. We conclude that Ca is time varying during the respiratory cycle.

Cause of the time-varying pulmonary arterial compliance. The cause of the time-varying Ca is most likely a passive mechanical effect, because our results did not relate the phenomenon to an active neurohumoral effect as we had anticipated initially. We found no effect of meclofenamate or vagotomy on the increase in Ca that occurs with inspiration. Although we cannot be certain that meclofenamate inhibited prostaglandin synthesis in the lung, lower dosages than we used (1–2 mg/kg) have been shown to virtually abolish renal efflux of prostaglandins (10). There is no doubt that the combination of atropine and vagotomy successfully blocked any vagal reflex. The fact that neither of the maneuvers affected the time variations of Ca suggests that passive rather than active mechanisms are involved.

Previously, we have shown that Ca can be separated into two components: elasticity and geometry (arterial dimensions; Ref. 7). Therefore, passive mechanical factors could cause Ca to be time varying as a result of time variation of pulmonary arterial elasticity or of pulmonary arterial blood volume. To our knowledge, there have been no previous reports that pulmonary arterial elasticity is time varying. There are, however, changes in the volume of both the alveolar and the extra-alveolar vessels that occur with alterations of lung volume (9). From their study, we would anticipate an increase in the volume of the extra-alveolar arteries and a decrease in the volume of the alveolar vessels with inspiration. The time variation of Ca cannot be explained simply on the basis of a change of lung volume because Ca increased only at SE but not at SI when lung volume was expanded by increased levels of PEEP. Nevertheless, the increase of Ca with inspiration may be related to the dynamic changes in vascular dimensions that must be occurring during positive-pressure ventilation. Although there have been no previous reports that pulmonary vascular elasticity is time varying, the variation in Ca need not be due to alterations of the elastic properties of the pulmonary arteries per se. Ca is estimated from data obtained under dynamic rather than static conditions. The

TABLE 2. *Effect of vagotomy on hemodynamic variables and their response to ventilation and positive end-expiratory pressure*

Hemodynamic Variables	Phase of Ventilation: Start of inspiration, cmH_2O PEEP 5	10	15	Start of expiration, cmH_2O PEEP 5	10	15	Effect of Vagotomy: V	V* VENT	V* PEEP	
PAP, cmH_2O										
B	30±3	32±2	34±2	30±2	31±2	34±2	<0.0001	NS	<0.0001	70
A	30±2	34±2	38±3	29±2	34±2	38±2				
$\dot{Q}$, l/min										
B	1.8±0.3	1.6±0.3	1.2±0.3	1.6±0.3	1.1±0.3	0.8±0.2	NS	NS	0.013	70
A	1.7±0.1	1.8±0.2	1.4±0.3	1.4±0.2	1.3±0.3	0.9±0.3				
Z_c, $dyn \cdot cm^{-5} \cdot s$										
B	188 + 18 − 16	161 + 7 − 7	157 + 17 − 15	178 + 12 − 11	161 + 12 − 11	168 + 16 − 14	NS	NS	NS	70
A	178 + 21 − 19	177 + 22 − 19	233 + 24 − 22	188 + 18 − 17	186 + 18 − 17	119 + 61 − 41				
Ca, 10^{-3} $dyn^{-1} \cdot cm^5$										
B	0.95 + 0.28 − 0.21	1.4 + 0.5 − 0.4	1.7 + 0.6 − 0.4	0.94 + 0.8 − 0.4	2.7 + 2.1 − 1.2	7.0 + 2.6 − 1.9	NS	NS	0.007	64
	1.7 + 0.6 − 0.4	1.1 + 0.3 − 0.3	1.1 + 0.3 − 0.2	4.2 + 4.6 − 2.2	1.6 + 0.8 − 0.6	1.1 + 0.1 − 0.1				
RVEDP, cmH_2O										
B	7±3	7±3	9±3	7±3	8±3	10±3	0.006	NS	NS	70
A	7±3	8±3	12±1	7±3	9±3	13±1				
HR, min^{-1}										
B	147±6	159±4	160±5	147±6	159±4	162±5	0.0006	NS	NS	70
A	152±6	164±6	180±5	152±6	164±5	182±5				
BP, mmHg										
B	125±4	114±10	88±15	126±4	112±9	88±15	<0.0001	NS	0.03	70
A	144±6	135±6	126±6	144±5	135±6	129±7				
SV, ml										
B	12±2	10±2	8±2	11±2	7±2	5±2	NS	NS	0.02	70
A	11±1	11±2	8±2	9±1	8±2	5±2				

Values are means ± SE and are given for before (B) and after (A) vagotomy. Hemodynamic variables are as defined in Table 1 footnote. *P* values are given for effect of vagotomy (V), effect of vagotomy on response to ventilation (V*VENT), and effect of vagotomy on response to PEEP (V*PEEP); *n*, no. of data points.

change in Ca may be related to a shift of blood volume within the pulmonary vasculature during the respiratory cycle.

At SE, the increased lung volume has the effect of increasing the size of the extra-alveolar vessels and compressing the capillary bed due to the increased alveolar pressure. At SI, the extra-alveolar vessels are smaller and the alveolar vessels are larger. Because expiration is passive, most of the change in lung volume occurs at the start of expiration when our measurements are made. At this juncture, there must be a shift of blood volume from the extra-alveolar arteries to the alveolar capillaries as a result of a simultaneous decrease of extra-alveolar arterial volume and an increase of alveolar capillary volume during expiration. This shift will result in an increase in the effective compliance of the pulmonary arterial tree. This explanation assumes that pulmonary vessels behave as pure elastic structures with a negligible viscous component. Although we know of no direct evidence of this for intrapulmonary vessels, it has been clearly demonstrated for the main pulmonary artery at cardiac frequency where there is no significant phase difference between changes of pressure and diameter (16). To test this explanation, it would be necessary to measure the longitudinal pressure gradient or instanteous flow between the extra-alveolar arteries and the alveolar vessels. We would anticipate that there would be an increase in this pressure gradient and flow at SE as blood is moved from the extra-alveolar arteries into the alveolar vessels.

Although we did not isolate a neurohumoral cause for the increased compliance with inspiration, we cannot exclude the possibility that some other mechanism is involved that was not tested in this study. We believe that the time-varying compliance could be explained by the well-established effect of respiratory motion on the alveolar and extra-alveolar vessels.

Consequences of a time-varying pulmonary arterial compliance. The nature of a lumped parameter model is to simplify the multiple components of a system into a few key elements. This process is achieved only at a price. By lumping Ca into one element, it is assumed that Ca can be considered as a time-invariant frequency-independent parameter. Determination of Ca at

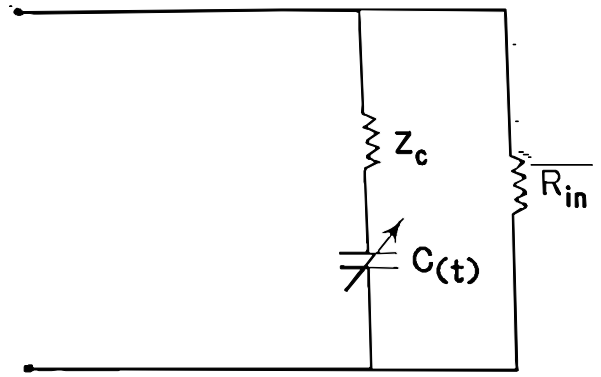

FIG. 5. Electrical representation of the pulmonary circulation with 2 resistors Rin and Z_c and a time-varying capacitor $C(t)$ to represent Ca.

different times during the ventilatory cycle is a test of time invariance. The results of this study indicate that Ca behaves as a time-varying quantity, which suggests that this assumption of time invariance is incorrect. For many applications, a lumped parameter model with time-invariant elements may be sufficient, depending on the subject of investigation. The problem of a time-varying Ca can be circumvented by making measurements of pressure and flow at a specified phase of the respiratory cycle. Alternatively, a time-varying compliance could be incorporated into the lumped parameter model used to represent pulmonary arterial input impedance.

An electrical representation with a time-varying compliance is shown in Fig. 5 and described in detail in the APPENDIX. The impedance of this network has some important consequences. First, the presence of a variable compliance suggests that the system can operate as a pump. A time-varying elastance (the reciprocal of compliance) is used, for example, to simulate ventricular function (14). The idea that pulmonary vasculature could behave like a pump was suggested over 40 years ago by Macklin (11). He noticed that there was an inflow of perfusate during inflation of the isolated lung. This demonstration of the pumping action of the lungs provides qualitative support for the existence of a time-varying compliance. He referred to the lung as the "pulmonic accessory heart." Second, the pulmonary vasculature could behave as if there is no resistance under two conditions: when Rin and Z_c are equal or when cardiac and respiratory frequencies are equal. Although the former may be difficult to achieve because of physiological limitations, the latter could be achieved by high-frequency ventilation. These results support the idea that high-frequency ventilation could be used to supplement cardiac function (12).

The beneficial effects of varying intrathoracic pressure in cardiac output have been considered to be mediated by modifying extracardiac pressure and the position of the interventricular septum (12). The present study leads us to suggest another possible mechanism: the cyclical variation of lung volume may force blood through the lungs due to its reciprocating effects on the extra-alveolar and the alveolar vascular volume. The pumping action of the lungs on the pulmonary vessels results in forward flow because the pulmonary and mitral valves prevent retrograde motion.

APPENDIX

Pulmonary arterial input impedance is represented by a three-element lumped parameter model (Fig. 5). Rin is a resistor that represents input resistance; Z_c is a resistor that represents characteristic impedance; $C(t)$ is a capacitance that represents the time-varying compliance. $C(t)$ is defined by the expression

$$C(t) = C_o + 2C_1 \cos \omega_R t \qquad (A1)$$

where C_o is the time-invariant portion of compliance and C_1 is the time-varying compliance that depends on the respiratory frequency, f_R. ω_R is $2\pi f_R$. The power source is the right ventricle, which operates at the frequency ω_H. Input impedance (Z_i) can be calculated by the expression

$$Z_i = \{[\omega_H C_1^2(\omega_H - \omega_R)(Z_c - Rin)]/[jC_o(\omega_H - \omega_R) \times (Z_c - Rin) + 1] + j\omega_H C_o\}^{-1} \qquad (A2)$$

where j is the square root of -1. When $Z_c = Rin$ or $\omega_H = \omega_R$, *Eq. A2* can be simplified as follows

$$Z_i = [j\omega_H C_o]^{-1} \qquad (A3)$$

Equation A3 indicates that Z_i has only an imaginary component and no real resistance under these special conditions.

We thank Amy Wurtenberger and Colleen Marx for expert technical assistance and Brenda Sauka for preparing the manuscript.

This work was supported by grants from the Whitaker Foundation, American Lung Association Research Fellowship (J. M. Fitzpatrick), and Research Career Development Award HL-01418 (B. J. B. Grant), Grant HL-41011, and Biomedical Research Support Grant S0-RR-07066 from the National Heart, Lung, and Blood Institute.

Address for reprint requests: B. J. B. Grant, ECMC (Pulmonary Div.), 462 Grider St., Buffalo, NY 14215.

Received 10 May 1990; accepted in final form 10 September 1990.

REFERENCES

1. BAIER, H., L. YERGER, R. MOAS, AND A. WANNER. Vascular and airway effects of endogenous cyclooxygenase products during lung inflation. *J. Appl. Physiol.* 59: 884–889, 1985.
2. BRIGHAM, E. O. Applying the discrete Fourier transform. In: *The Fast Fourier Transform.* Englewood Cliffs, NJ: Prentice-Hall, 1974, p. 132–146.
3. CALVIN, J. E., JR., R. W. BAER, AND S. A. GLANTZ. Pulmonary artery constriction produces greater right ventricular dynamic afterload than lung microvascular injury in the open chest dog. *Circ. Res.* 56: 40–56, 1985.
4. CASSIDY, S. S., W. L. ESCHENBACHER, AND R. L. JOHNSON, JR. Reflex cardiovascular depression during unilateral lung hyperinflation in the dog. *J. Clin. Invest.* 64: 620–626, 1979.
5. FISHMAN, A. P. Pulmonary circulation. In: *Handbook of Physiology. The Respiratory System. Circulation and Nonrespiratory Functions.* Bethesda, MD: Am. Physiol. Soc., 1985, sect. 3, vol. I, chapt. 3, p. 93–165.
6. FITZPATRICK, J. M., AND B. J. B. GRANT. Effect of pulmonary embolism on right ventricular afterload (Abstract). *Am. Rev. Respir. Dis.* 135: A304, 1989.
7. GRANT, B. J. B., AND J. M. CANTY, JR. Effect of cardiac output on pulmonary hemodynamics. *Respir. Physiol.* 79: 303–318, 1989.
8. GRANT, B. J. B., AND L. J. PARADOWSKI. Characterization of pulmo-

nary arterial input impedance with lumped parameter models. *Am. J. Physiol.* 252 (*Heart Circ. Physiol.* 21): H585–H593, 1987.
9. HOWELL, J. B. L., S. PERMUTT, D. F. PROCTOR, AND R. L. RILEY. Effect of inflation of the lung on different parts of the pulmonary vascular bed. *J. Appl. Physiol.* 16: 71–76, 1961.
10. LONIGRO, A. J., H. D. ITSKOVITZ, K. CROWSHAW, AND J. MCGIFF. Dependency of renal blood flow on prostaglandin synthesis in the dog. *Circ. Res.* 32: 712–717, 1973.
11. MACKLIN, C. C. Evidences of the capacity of the pulmonary arteries and veins of dogs, cats and rabbits during inflation of the freshly excised lung. *Rev. Can. Biol.* 5: 199–232, 1946.
12. MATUSCHAK, G. M., M. R. PINSKY, AND M. KLAIN. Hemodynamic effects of synchronous high-frequency jet ventilation during hypovolemia. *J. Appl. Physiol.* 61: 44–53, 1986.
13. MILNOR, W. R. Arterial impedance as ventricular afterload. *Circ. Res.* 36: 565–570, 1975.
14. MILNOR, W. R. Cardiac dynamics. In: *Hemodynamics.* Baltimore, MD: Williams & Wilkins, 1989, p. 260–293.
15. MURGO, J. P., AND N. WESTERHOF. Input impedance of the pulmonary arterial system in normal man. *Circ. Res.* 54: 666–673, 1984.
16. PATEL, D. J., D. P. SCHILDER, AND A. J. MALLOS. Mechanical properties and dimensions of the major pulmonary arteries. *J. Appl. Physiol.* 15: 92–96, 1960.
17. PRESS, W. H., B. P. FLANNERY, S. A. TEUKOLSKY AND W. T. VETTERLING. Modeling of data. In: *Numerical Recipes.* Cambridge, UK: Cambridge Univ. Press, 1986, p. 498–546.
18. POULEUR, H., J. LEFEVRE, C. H. VAN EYLL, P. M. JAUMIN, AND A. A. CHARLIER. Significance of pulmonary input impedance in right ventricular performance. *Cardiovasc. Res.* 12: 617–629, 1978.
19. ROBERTS, A. M., H. M. COLERIDGE, AND J. C. G. COLERIDGE. Reciprocal action of pulmonary vagal afferents on tracheal smooth muscle tension in dogs. *Respir. Physiol.* 72: 35–46, 1988.
20. VAN DEN BOS, G. C., N. WESTERHOF, AND O. S. RANDALL. Pulse wave reflection: can it explain the differences between systemic and pulmonary pressure and flow waves? *Circ. Res.* 51: 479–485, 1982.